

Received December 1, 2020, accepted December 17, 2020, date of publication December 21, 2020, date of current version January 8, 2021.

Digital Object Identifier 10.1109/ACCESS.2020.3046192

# A New Family of Step-Up Hybrid Switched-Capacitor Integrated Multilevel Inverter Topologies With Dual Input Voltage Sources

ATIF IQBAL<sup>ID</sup>, (Senior Member, IEEE), MARIF DAULA SIDDIQUE<sup>ID</sup>, (Member, IEEE),  
B. PRATHAP REDDY<sup>ID</sup>, (Member, IEEE), PANDAV KIRAN MAROTI<sup>ID</sup>, (Member, IEEE),  
AND RASHID ALAMMARI<sup>ID</sup>, (Senior Member, IEEE)

Department of Electrical Engineering, Qatar University, Doha, Qatar

Corresponding author: Marif Daula Siddique (marif.daula@qu.edu.qa)

This work was supported by the Qatar University-Marubeni Concept to Prototype Development Research grant # [MCTP-CENG-2020- 2] from the Qatar University and the publication charges (APC) is paid by the Qatar National Library, Doha, Qatar.

**ABSTRACT** In the low voltage based renewable systems like PV and Fuel cell applications, the step-up of the output voltage to drive the loads is essential. For this, the integration of switched-capacitor (SC) units with the dc-ac converters will have the potential advantages like improved efficiency, optimal switching devices, small size of passive elements (L and C) as compared with traditional two-stage conversion system (dc/dc converter and dc/ac converter). This paper focuses on a new family of step-up multilevel inverter topologies with switched capacitor integration with dual input voltage sources. With the flexibility of 2 dc sources and switching capacitor circuits, four different topologies have been suggested in this paper with features of high voltage gain, reduced component count, reduced voltage stress and self-voltage balancing of the capacitor while achieving a higher number of levels. A detailed analysis of proposed multilevel inverters has been analyzed with the symmetrical and asymmetrical mode of operations and the associated gain, the number of levels, and other performance indices are presented. An in-depth study of all the topologies has been accomplished in this paper with several comparative studies in terms of components count, voltage gain and cost. The effectiveness and practicability of the suggested topology with 13 level output voltage has been explained by the experimental results obtained from a scale down prototype.

**INDEX TERMS** Hybrid reduced switch bidirectional cascaded H-bridge multilevel inverter, pulse width modulation (PWM), total harmonics distortion (THD).

## I. INTRODUCTION

With the rising demand for renewable energy sources, the importance of multilevel inverters (MLI) has been at its peak for the dc-ac power conversion. The growing application of MLIs in the renewable energy system is due to the advantages of connecting several dc-link formed by dc voltage sources. The string of dc voltage sources can comprise multiple solar photovoltaic (PV) units, ultra-capacitors, or batteries to get different voltage levels. The MLI can integrate these dc power sources to achieve an efficient dc/ac power conversion for high voltage applications. Multilevel inverters also demonstrate the properties like improved output parameters (like reduced harmonic distortion, improved fundamental

voltage), reduced the size of the required filter, reduced voltage rating of individual switches, and improved efficiency. The traditional MLI configurations have been categorized as neutral point clamped (NPC), flying capacitor (FC), and cascaded H-bridge (CHB) with their different evolved structures. Conversely, with traditional topologies, the component count is high for a higher level count of output voltage. Further, they also suffer from capacitor voltage balancing issue [1]–[3]. The research related to MLIs has been done from the last four to five decades and still, there is a research scope on MLI topologies and their control with the advanced features like simple in realization, higher fault tolerance, hybrid single state for low voltage dc to high voltage dc and many more. The current research related to MLI has been the reduced component count topologies with modularity, reduced voltage stresses, higher efficiency, etc., [4]–[7].

The associate editor coordinating the review of this manuscript and approving it for publication was Sanjeevikumar Padmanaban<sup>ID</sup>.

Based on the reduced switch count, numerous topologies have been proposed [3], [8]. The optimal design of several topologies has also been considered to reduce the number of switches and dc voltage source count [9]–[11]. However, the main issue with these topologies has been the requirement of a higher number of isolated dc voltage sources, which makes them not suitable for practical applications. Another drawback of these topologies has been the lacking of boosting the input voltage.

The integration of capacitors in the multilevel inverter topology is not a new concept as capacitors have been used in NPC and FC based MLIs. However, the capacitor used in these topologies does not provide any boosting feature. In recent years, the switched-capacitor based multilevel inverter (SCMLI) topologies based on series/parallel combination of capacitors have gained much popularity for high voltage applications [12]–[16]. This is due to the boosting feature possess by the SCMLI. The self-voltage balancing of the capacitors is the additional important feature of the SC-based topology which reduces the control complexity of the system. The step-up or boosting feature enables the low voltage sources such as PV systems to be used for the high voltage applications. These step-up converters eliminate the need for intermittent boost dc/dc converter topology, results in lower size and cost with improved efficiency of the overall system. However, the higher number of components and their extension for a higher number of levels have been the major challenges nowadays. A seven-level topology has been proposed in [17], which uses 16 switches with two capacitors. Similarly, nine-level topologies have been proposed in [18], [19], which uses 11 and 12 switches respectively. However, for a higher number of levels, the only option is the cascade connection of several modules which increases the components count.

Apart from a large number of components required for a higher number of levels, another problem associated with the SC-MLI topologies has been the lower power ranges due to the high current rating of some of the switches [20]. The problem of lower power rating can be solved by having multiple dc voltage sources with SC modules. The use of multiple dc voltage sources splits the amount of current among the available dc voltage sources and switches. Several topologies with multiple sources based on SC-MLI have been reported in the literature. A topology with a higher number of levels has been recommended in [20], however, due to the higher number of components, reliability has been one of the major issues. Another topology with 13 level output voltage has been proposed in [21], which uses 14 switches with two capacitors of different voltage ratings. Furthermore, in the topology of [21], the charging time for both capacitors is very less compared to their discharging time, which leads to a higher voltage ripple of the capacitor voltages. A nine-level dual input topology has been proposed in [2], however, it lacks the boosting feature along with higher total standing voltage (TSV) due to the use of backend H-bridge for the purpose of polarity change across the load. Similarly, some

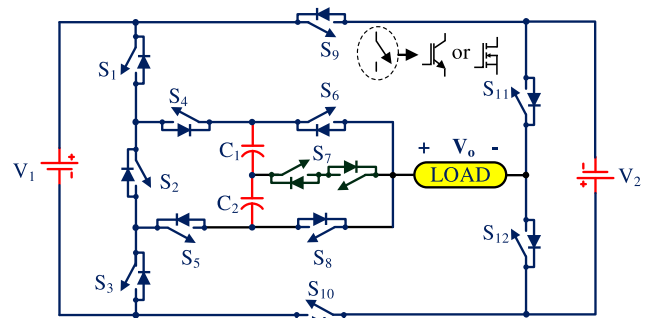


FIGURE 1. First proposed topology (PT-I).

more topologies with multiple dc voltage sources have been proposed in [2], [21]–[31].

In this paper, a new family of dual input SC-MLI has been proposed to achieve a higher number of voltage levels ensuring the lower number of components and TSV. The proposed topologies provide the boosting of the input voltage. The paper has been organized as follows: Section II gives a detailed explanation of the suggested topology in both symmetrical and asymmetrical configurations. In Section III, a comparison of different topologies has been provided and Section IV gives the experimental results. The conclusion of the paper is given in Section V.

## II. PROPOSED DUAL SOURCE TOPOLOGIES

### A. PROPOSED TOPOLOGY-I (PT-I)

The assembly of the 1<sup>st</sup> proposed topology is shown in Fig. 1. It consist of two dc voltage source  $V_1$  and  $V_2$  and 12 switches. The two capacitors  $C_1$  and  $C_2$  are integrated with the dc voltage source  $V_1$  and give the boosting feature to the proposed topology. Both capacitors are charged by connecting them in parallel to the dc voltage source  $V_1$ . However, 19 different combinations are available from the topology shown in Fig. 1. The switching table for different switching states is given in Table 1 with the charging and discharging state of both capacitors. Based on Table 1, the different positive voltage states of the proposed topology I are illustrated in Fig. 2 (a)-(j).

Another important aspect of the proposed topology has been reduced voltage stress. The maximum peak voltage of different switches are given as

$$\left. \begin{aligned} V_{S1} &= V_{S2} = V_{S3} = V_{S4} = V_{S5} = V_{S6} = V_{S8} = V_1 \\ V_{S7} &= 0.5V_1 \\ V_{S9} &= V_{S10} = V_1 + V_2 \\ V_{S11} &= V_{S12} = V_2 \end{aligned} \right\} (1)$$

Therefore the TSV of the PT-I can be calculated as

$$TSV = \sum_{x=1}^{12} V_{sx} = 10V_1 + 4V_2 \quad (2)$$

As it is clear from Table 1, the PT-I can produce a maximum of 19 levels of the output voltage. The magnitude of both dc voltage sources  $V_1$  and  $V_2$  of the PT-I can be selected in two different modes of operation, i.e., symmetrical and asymmetrical.

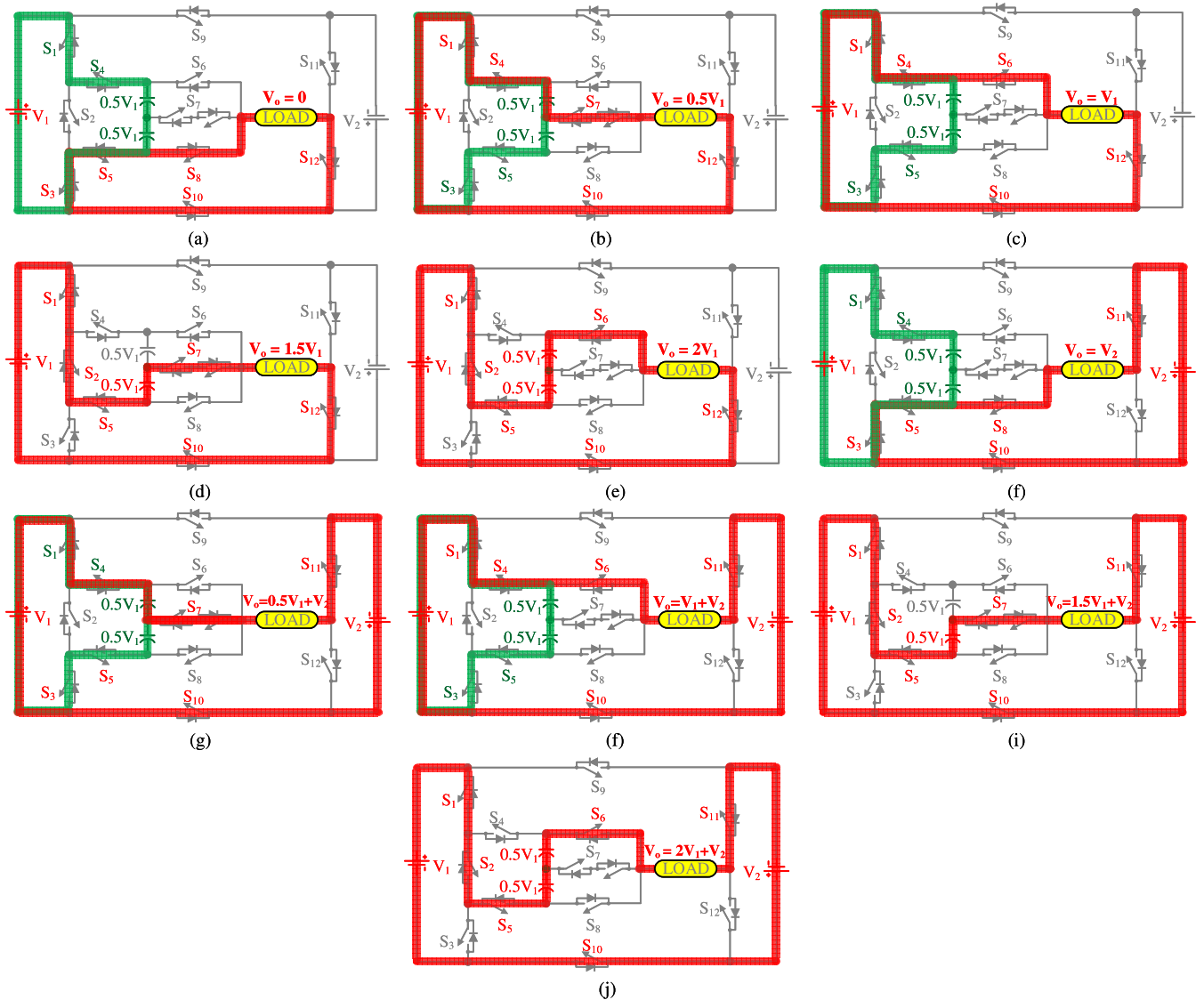


**FIGURE 2.** All possible voltage states of the proposed topology I with (a)  $V_o = 0$ , (b)  $V_o = 0.5V_1$ , (c)  $V_o = V_1$ , (d)  $V_o = 1.5V_1$ , (e)  $V_o = 2V_1$ , (f)  $V_o = V_2$ , (g)  $V_o = 0.5V_1 + V_2$ , (h)  $V_o = V_1 + V_2$ , (i)  $V_o = 1.5V_1 + V_2$ , (j)  $V_o = 2V_1 + V_2$ .

1) SYMMETRICAL MODE

In this mode, the magnitude of both dc voltage sources is selected as  $V_{dc}$ , i.e.  $V_1 = V_2 = V_{dc}$ . With this selection, the capacitor voltages are changed up to half of  $V_1$ , i.e.,  $0.5V_{dc}$ . Therefore, in this mode, the total number of voltage levels which can be generated becomes 13 with peak output voltage,  $V_{o,peak} = 3V_{dc}$ . With  $V_1 = V_2 = V_{dc}$ , the TSV of the proposed topology I become  $14V_{dc}$ , the per-unit TSV (TSV<sub>pu</sub>) can be calculated as

$$TSV_{pu} = \frac{TSV}{V_{o,peak}} = \frac{14V_{dc}}{3V_{dc}} = 4.67 \tag{3}$$

The voltage gain (VG) can be calculated as

$$VG = \frac{V_{o,peak}}{V_1 + V_2} = \frac{3V_{dc}}{2V_{dc}} = 1.5 \tag{4}$$

2) ASYMMETRICAL MODE

In this mode, the magnitude of both dc voltage sources has a different magnitude. For generating the maximum number of levels with a maximum voltage gain, the magnitude of  $V_1$  is kept higher than the magnitude of  $V_2$ . With these criteria, the magnitude of both voltage sources i.e.,  $V_1$  and  $V_2$  are selected as  $4V_{dc}$  and  $V_{dc}$  respectively. With this magnitude selection, both capacitor voltages attend a maximum of  $2V_{dc}$ . The TSV and  $V_{o,peak}$  becomes  $44V_{dc}$  and  $9V_{dc}$  respectively. the TSV<sub>pu</sub> and VG are calculated from (3) and (4) as

$$\left. \begin{aligned} TSV_{pu} &= \frac{44V_{dc}}{9V_{dc}} = 4.89 \\ VG &= \frac{9V_{dc}}{5V_{dc}} = 1.8 \end{aligned} \right\} \tag{5}$$

Therefore, with asymmetrical mode, the number of levels is increased to 19 with a higher voltage gain of 1.8.

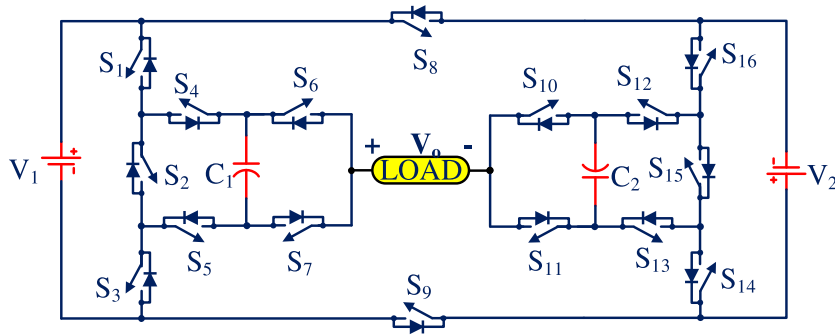


FIGURE 3. Circuit configuration of PT-II.

TABLE 1. Switching state of the proposed topology-I.

S <sub>1</sub>	S <sub>2</sub>	S <sub>3</sub>	S <sub>4</sub>	S <sub>5</sub>	S <sub>6</sub>	S <sub>7</sub>	S <sub>8</sub>	S <sub>9</sub>	S <sub>10</sub>	S <sub>11</sub>	S <sub>12</sub>	V <sub>0</sub>	V <sub>C1</sub>	V <sub>C2</sub>
1	0	1	1	1	0	0	1	0	1	0	1	0	C	C
1	0	1	1	1	0	1	0	0	1	0	1	0.5V <sub>1</sub>	C	C
1	0	1	1	1	1	0	0	0	1	0	1	V <sub>1</sub>	C	C
1	1	0	0	1	0	1	0	0	1	0	1	1.5V <sub>1</sub>	-	D
1	1	0	0	1	1	0	0	0	1	0	1	2V <sub>1</sub>	D	D
1	0	1	1	1	0	0	1	0	1	1	0	V <sub>2</sub>	C	C
1	0	1	1	1	0	1	0	0	1	1	0	0.5V <sub>1</sub> +V <sub>2</sub>	C	C
1	0	1	1	1	1	0	0	0	1	1	0	V <sub>1</sub> +V <sub>2</sub>	C	C
1	1	0	0	1	0	1	0	0	1	1	0	1.5V <sub>1</sub> +V <sub>2</sub>	D	-
1	1	0	0	1	1	0	0	0	1	1	0	2V <sub>1</sub> +V <sub>2</sub>	D	D
1	0	1	1	1	1	0	0	1	0	1	0	0	C	C
1	0	1	1	1	0	1	0	1	0	1	0	-0.5V <sub>1</sub>	C	C
1	0	1	1	1	0	0	1	1	0	1	0	-V <sub>1</sub>	C	C
0	1	1	1	0	0	1	0	1	0	1	0	-1.5V <sub>1</sub>	D	-
0	1	1	1	0	0	0	1	1	0	1	0	-2V <sub>1</sub>	D	D
1	0	1	1	1	1	0	0	1	0	0	1	-V <sub>2</sub>	C	C
1	0	1	1	1	0	1	0	1	0	0	1	-(0.5V <sub>1</sub> +V <sub>2</sub> )	C	C
1	0	1	1	1	0	0	1	1	0	0	1	-(V <sub>1</sub> +V <sub>2</sub> )	C	C
0	1	1	1	0	0	1	0	1	0	0	1	-(1.5V <sub>1</sub> +V <sub>2</sub> )	-	D
0	1	1	1	0	0	0	1	1	0	0	1	-(2V <sub>1</sub> +V <sub>2</sub> )	D	D

**B. PROPOSED TOPOLOGY II (PT-II)**

In PT-I, the switched capacitor units are connected to the dc voltage source V<sub>1</sub> which results in the lower voltage gain and is limited to 1.8. To increase the VG, PT-I is modified by integrating two switched capacitor unit with both dc voltage sources and is depicted in Fig. 3. By adding two SC units, the switching Table for PT-II is given in Table 2. Similar to PT-I, the expression for TSV and V<sub>o,peak</sub> comes out to be

$$\left. \begin{aligned} TSV &= 9V_1 + 9V_2 \\ V_{o,peak} &= 2(V_1 + V_2) \end{aligned} \right\} \quad (6)$$

Similar to PT-I, the PT-II can be operated in two modes as the symmetrical and asymmetrical modes. In symmetrical mode, V<sub>1</sub> = V<sub>2</sub> = V<sub>dc</sub>. This results in the charging of both capacitors up to a voltage level of V<sub>dc</sub>. A maximum of nine levels can be generated with the symmetrical mode

of operation of PT-II. With a similar expression of PT-I, the different parameters for PT-II are given as

$$\left. \begin{aligned} TSV_{pu} &= \frac{18V_{dc}}{4V_{dc}} = 4.5 \\ VG &= \frac{4V_{dc}}{2V_{dc}} = 2 \end{aligned} \right\} \quad (7)$$

Furthermore, for the asymmetrical mode, considering a higher number of levels, the magnitude of V<sub>1</sub> and V<sub>2</sub> can be selected as 3V<sub>dc</sub> and V<sub>dc</sub> respectively. With this selection of magnitudes, 17 levels can be achieved across the load. The different parameters for the PT-II with the symmetrical mode of operation are given as

$$\left. \begin{aligned} TSV_{pu} &= \frac{36V_{dc}}{8V_{dc}} = 4.5 \\ VG &= \frac{8V_{dc}}{4V_{dc}} = 2 \end{aligned} \right\} \quad (8)$$

Based on PT-I and PT-II, two more hybrid topologies have been proposed in this paper which is depicted in Fig. 4 and termed as proposed topology-III (PT-III) and proposed topology-IV (PT-IV). Table 3 gives the summarized overview of all the proposed topology by considering both modes of operation.

**III. COMPARATIVE ANALYSIS**

In Table 4, a comparison of the proposed converter with recently existing converters is presented. The comparison has been done based on the number of components, voltage stress, voltage gain, and cost function. Based on this table, it can be noted that with asymmetrical configuration, the boosting factor of the proposed topology is higher than the topologies presented in [2] and [26]. It can be noted that the topologies presented in [2], and [26] generated 11 and 13 levels of output voltage using two dc voltage source with asymmetrical configuration, whereas for the proposed topology, 19 levels can be achieved. Further, the topology of [26] higher per unit TSV as compared to the proposed structure.

In addition to the component comparison, a cost function (CF) has been defined which has been used to evaluate different topologies of Table 4. The cost function and normalized CF (NCF) has been defined as [32]

$$\left. \begin{aligned} CF &= (N_{sw} + N_{gd} + N_d + N_C + \alpha \times TSV_{pu}) \times N_{dc} \\ NCF &= \frac{CF}{N_L} \end{aligned} \right\} \quad (9)$$

TABLE 2. Switching state of the proposed topology II.

S <sub>1</sub>	S <sub>2</sub>	S <sub>3</sub>	S <sub>4</sub>	S <sub>5</sub>	S <sub>6</sub>	S <sub>7</sub>	S <sub>8</sub>	S <sub>9</sub>	S <sub>10</sub>	S <sub>11</sub>	S <sub>12</sub>	S <sub>13</sub>	S <sub>14</sub>	S <sub>15</sub>	S <sub>16</sub>	V <sub>o</sub>	V <sub>C1</sub>	V <sub>C2</sub>
1	0	1	1	1	0	1	0	1	0	1	1	1	1	0	1	0	C	C
1	0	1	1	1	1	0	0	1	0	1	1	1	1	0	1	V <sub>1</sub>	C	C
1	1	0	0	1	1	0	0	1	0	1	1	1	1	0	1	2V <sub>1</sub>	D	C
1	0	1	1	1	0	1	0	1	1	0	1	1	1	0	1	V <sub>2</sub>	C	C
1	0	1	1	1	0	1	0	1	1	0	0	1	0	1	1	2V <sub>2</sub>	C	D
1	0	1	1	1	1	0	0	1	1	0	1	1	1	0	1	V <sub>1</sub> +V <sub>2</sub>	C	C
1	1	0	0	1	1	0	0	1	1	0	1	1	1	0	1	2V <sub>1</sub> +V <sub>2</sub>	D	C
1	0	1	1	1	1	0	0	1	1	0	0	1	0	1	1	V <sub>1</sub> +2V <sub>2</sub>	C	D
1	1	0	0	1	1	0	0	1	1	0	0	1	0	1	1	2V <sub>1</sub> +2V <sub>2</sub>	D	D
1	0	1	1	1	1	0	1	0	1	0	1	1	1	0	1	0	C	C
1	0	1	1	1	0	1	1	0	1	0	1	1	1	0	1	-V <sub>1</sub>	C	C
0	1	1	1	0	0	1	1	0	1	0	1	1	1	0	1	-2V <sub>1</sub>	D	C
1	0	1	1	1	1	0	1	0	0	1	1	1	1	0	1	-V <sub>2</sub>	C	C
1	0	1	1	1	1	0	1	0	0	1	1	0	1	1	0	-2V <sub>2</sub>	C	D
1	0	1	1	1	0	1	1	0	0	1	1	1	1	0	1	-(V <sub>1</sub> +V <sub>2</sub> )	C	C
0	1	1	1	0	0	1	1	0	0	1	1	1	1	0	1	-(2V <sub>1</sub> +V <sub>2</sub> )	D	C
1	0	1	1	1	0	1	1	0	0	1	1	0	1	1	0	-(V <sub>1</sub> +2V <sub>2</sub> )	C	D
0	1	1	1	0	0	1	1	0	0	1	1	0	1	1	0	-(2V <sub>1</sub> +2V <sub>2</sub> )	D	D

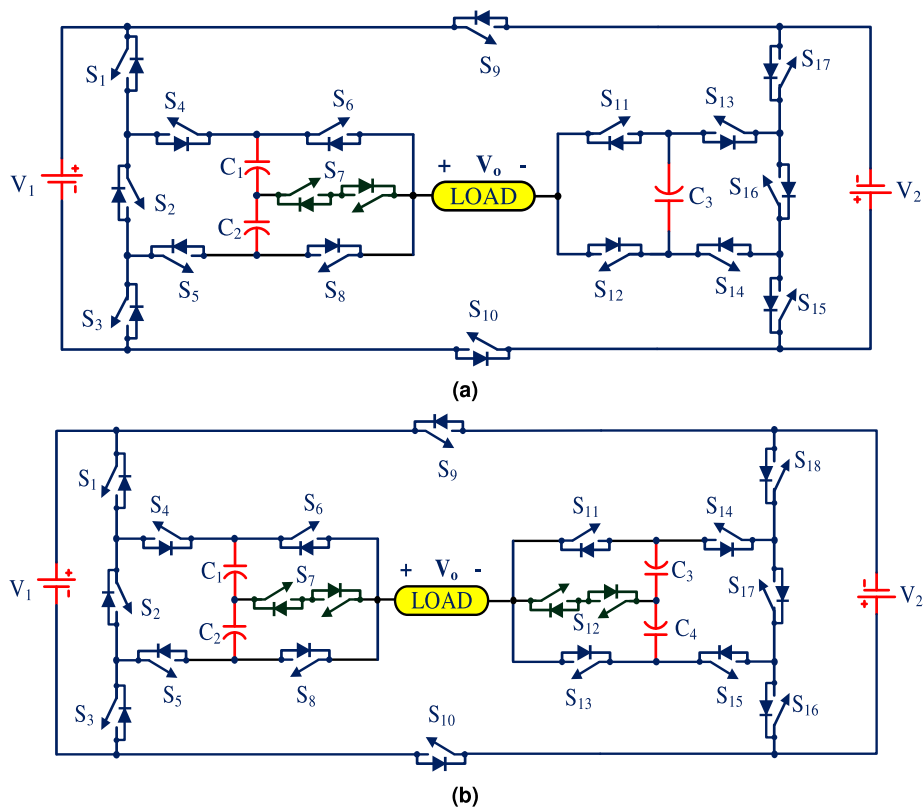


FIGURE 4. Schematic diagram of (a) PT-III and (b) PT-IV.

where  $\alpha$  is constant which is associated with the voltage stress of the topologies. From Table 4, it can be observed that the proposed structure with asymmetrical configurations

provides the lowest NCF for all values of  $\alpha$ . This signifies that the suggested arrangement is more cost-effective as compared to other suggested topologies. The proposed converter

TABLE 3. Different parameters of the proposed topologies.

PT	N <sub>sw</sub>	N <sub>gd</sub>	N <sub>C</sub>	Mode of operation	Magnitude of		N <sub>L</sub>	TSV <sub>pu</sub>	VG
					V <sub>1</sub>	V <sub>2</sub>			
I	13	12	2	Symmetrical	V <sub>DC</sub>	V <sub>DC</sub>	13	4.67	1.5
				Asymmetrical	4V <sub>DC</sub>	V <sub>DC</sub>	19	4.89	1.8
II	16	16	2	Symmetrical	V <sub>DC</sub>	V <sub>DC</sub>	9	4.5	2
				Asymmetrical	3V <sub>DC</sub>	V <sub>DC</sub>	17	4.5	2
III	18	17	3	Symmetrical	V <sub>DC</sub>	V <sub>DC</sub>	17	4.75	2
				Asymmetrical	V <sub>DC</sub>	2.5V <sub>DC</sub>	29	4.64	2
IV	20	18	4	Symmetrical	V <sub>DC</sub>	V <sub>DC</sub>	17	5	2
				Asymmetrical	5V <sub>DC</sub>	V <sub>DC</sub>	49	5	2

N<sub>sw</sub>/N<sub>gd</sub>/N<sub>C</sub>/N<sub>L</sub>= Number of switches / gate driver circuits/ capacitors / levels

TABLE 4. Comparison of PT-I with the other SCMLI topologies.

Topology	N <sub>L</sub>	N <sub>dc</sub>	N <sub>sw</sub>	N <sub>gd</sub>	N <sub>d</sub>	N <sub>C</sub>	TSV <sub>pu</sub>	VG	α=0.5		α=1.0		α=1.5		
									CF	NCF	CF	NCF	CF	NCF	
[2]	11	2	11	11	0	1	4.4	1.67	50.4	4.58	54.8	4.98	59.2	5.38	
[21]	13	2	14	11	0	2	5.33	2	59.3	4.56	64.66	4.97	69.99	5.38	
[23]	17	2	10	10	2	2	5.5	2	53.5	3.15	59	3.47	64.5	3.79	
[25]	17	2	10	10	2	2	5.5	2	53.5	3.15	59	3.47	64.5	3.79	
[26]	13	2	11	10	1	1	6.3	1.5	52.3	4.75	58.6	5.33	64.9	5.9	
[29]	13	2	18	15	0	2	5	2	75	5.77	80.0	6.15	85	6.54	
[30]	17	2	18	14	2	4	6	2	82	4.82	88.0	5.17	94	5.53	
[31]	19	2	12	12	6	4	5.8	2.25	73.8	3.88	79.6	4.19	85.4	4.50	
[PT-I]	Symmetrical	13	2	13	12	0	2	4.67	1.5	58.67	4.51	63.34	4.87	68.01	5.23
	Asymmetrical	19						4.89	1.8	58.89	3.10	63.78	3.36	68.67	3.61

provides a viable solution to achieve a high number of levels compared to other existing topologies with low voltage stress across the switches.

IV. RESULTS AND DISCUSSION

A. SIMULATION RESULTS

The symmetrical operation of the proposed topology, i.e., with V<sub>1</sub> = V<sub>2</sub> = 60V has been simulated using MATLAB software. A sinusoidal level-shifted carrier-based PWM with 12 carriers of 5kHz and one sinusoidal reference is implemented to attain the 13-level output voltage. The modulation index is the ratio of reference magnitude (V<sub>ref</sub>) to carrier reference (V<sub>carrier</sub>) and the output voltage of a proposed MLI is, V<sub>0</sub> = MI × (2V<sub>1</sub> + V<sub>2</sub>). The peak magnitude of the output voltage with MI = 1.0 is 180V with the symmetrical configuration of the source. Fig. 5 (a) depicts the output waveforms of the load voltage, current and both capacitor voltage with a change of load parameter. At the time, t = 0.1s, the load is changed from 90Ω to 80mH + 90Ω, the nature of load current changes, however, both capacitor voltage remains balanced. Similarly, Fig. 5 (b) illustrates the different waveforms with the change of MI from 0.80 to 0.90 to 1.0. With lower MI, the magnitude of the output voltage reduces.

However, the capacitor voltages remain balanced with the change of MI. Furthermore, Fig. 6 (a) and (b) illustrate the voltage and current stress of all 12 switches with a load parameter of 80mH + 90Ω. Out of 13 switches, S<sub>1</sub>-S<sub>6</sub>, S<sub>8</sub>, S<sub>11</sub>, and S<sub>12</sub> need to be of a voltage rating of 100V, switches S<sub>9</sub> and S<sub>10</sub> need to of voltage rating of 200V and the remaining two switches of the bidirectional switch S<sub>7</sub> need to block the voltage of 30V. In the charging loop of both capacitors, four switches are present, i.e., S<sub>1</sub>, S<sub>3</sub>, S<sub>4</sub> and S<sub>5</sub> need to of the current rating which is equal to the sum of changing and load current. The remaining switches of the topology have a current rating equal to the load current.

B. EXPERIMENTAL RESULTS

The experimental prototype of the proposed switched-capacitor multilevel inverter as shown in Fig. 7, has built-in the laboratory with the following: G60N100 IGBT switches, TDK Lambda GEN300-11 DC regulated power supplies, RL load Banks, PG6DI (450V and 2200μF) capacitors, FPGA Vertix-5 (XC5VLX50T) controller and GDA-2A4S1 Gate Drivers. The proposed MLI configuration is tested at 50Hz/5kHz modulating/switching fre-



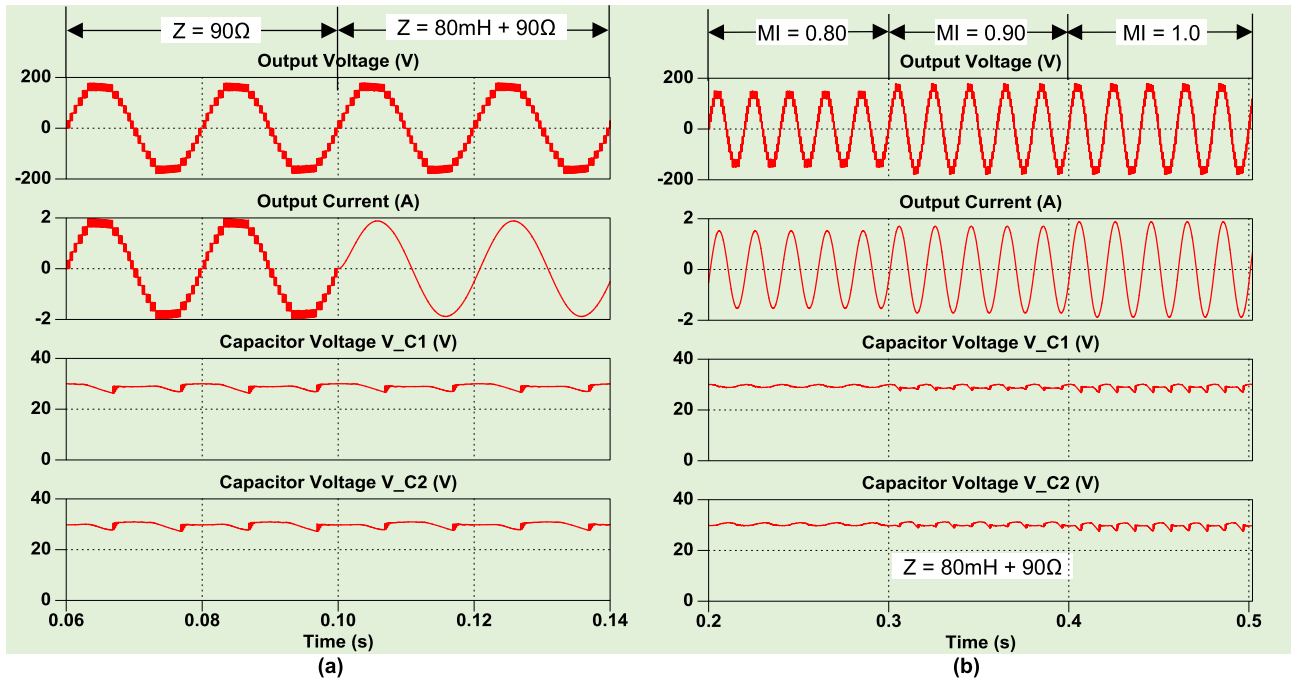


FIGURE 5. Simulation results with change of (a) load and (b) MI.

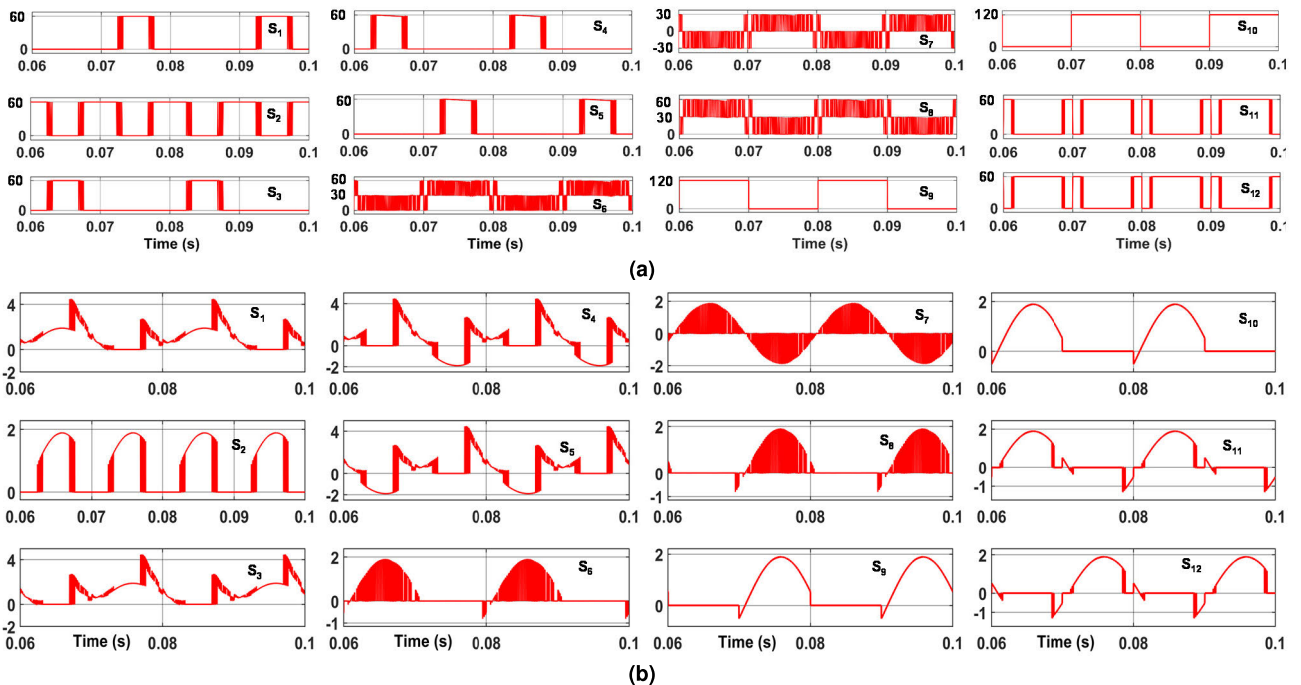


FIGURE 6. Simulation results of (a) voltage stress and (b) current stress of switches with symmetrical configuration.

quency, two 60V power supplies, two 90Ω load resistors and two 80mH load inductors. From the switching logic given in Table. 1, the complementary switch pair gate pulses are controlled with a 2μs delay to avoid the short circuit of source/load/capacitors. The control logic for symmetrical

DC source driven proposed MLI is implemented in FPGA Vertex-5 board, where the programming has done in VHDL language. The proposed multilevel inverter is tested at various operating conditions, i.e., R load, RL load, a Step change in R/RL loads, Change of load type i.e., R to RL type, Change

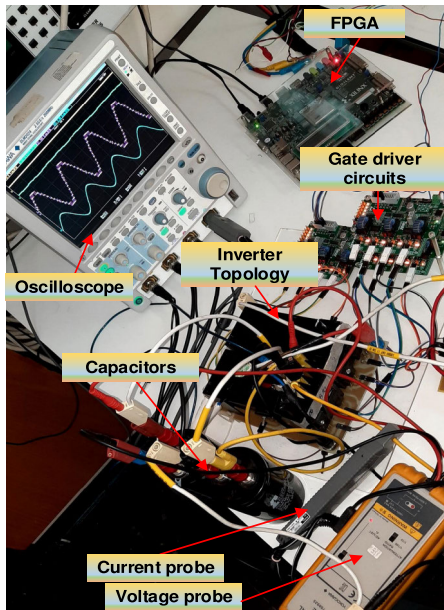


FIGURE 7. Experimental Setup.

of modulation index (MI) values, and Change of frequency of output voltage. These test results are evident for an effective operation of the proposed symmetrical source driven 13-level step-up boost inverter.

Fig. 8 shows the waveforms of 13 level output voltage, and voltage stress of switches ( $S_1, S_5$ ) and ( $S_3, S_4$ ). With the magnitude of  $V_1 = V_2 = 60V$ , the peak of the output voltage is 180V. The voltage stress of switches ( $S_1, S_5$ ) and ( $S_3, S_4$ ) have a peak magnitude of 60V, which is equal to the dc source magnitude. Similarly, Fig. 9 (a) illustrates the voltage stress of switches  $S_9, S_{10}$ , and  $S_{12}$ . The switches  $S_9$  and  $S_{10}$  have

maximum voltage stress which is equal to the sum of the input voltage, i.e., 120V. The maximum voltage stress for switches  $S_{12}$  is 60V.

The proposed MLI with Resistive (R) load ( $90 \Omega$ ) is tested in a laboratory for a MI = 1.0, and the associated test results are given in Fig. 9 (b). In this waveform, capacitor voltages, output voltage, and output current have been shown. Here the capacitors are charged symmetrically with half the voltage of DC-link voltage, i.e.,  $V_{C1} = V_{C2} = 30V$ . Since the load is a Resistive type, the output voltage and current are in phase and having the same wave shape (13 level voltage). The peak output voltage and current of symmetrical DC source driven proposed MLI are 180V and 2A respectively. From these voltage/current waveforms, it is observed that the levels symmetrical and each voltage level is a step of 30V. The experimental analysis of proposed MLI is also carried out for Resistive-Inductive (RL) load at MI = 1, the results are shown in Fig. 9 (c). In this figure, it is observed that the current is sinusoidal and it is lagging behind the phase voltage since the load is inductive in nature. The peak voltage and current magnitudes are 180V/2A and the capacitor voltages are balanced (30V). Fig. 9 (d) demonstrates the harmonic spectrum of the 13 level output voltage waveform. The THD content of the output voltage is 8.9%. The lower order harmonics are almost zero due to the switching frequency of 5kHz which reduces the filter requirement.

The proposed MLI is tested under step change in Resistive load and the respective results are presented in Fig. 10. To show the effectiveness of a proposed MLI, a step-change in RL load is done and the associated results are presented in Fig. 10. In this figure, the enlarged version of experimental results for a step change of RL load, i.e., no-load to  $180\Omega$ -180mH and  $180\Omega$ -180mH to  $90\Omega$ -90mH are presented. The step-change in R load has been demonstrated

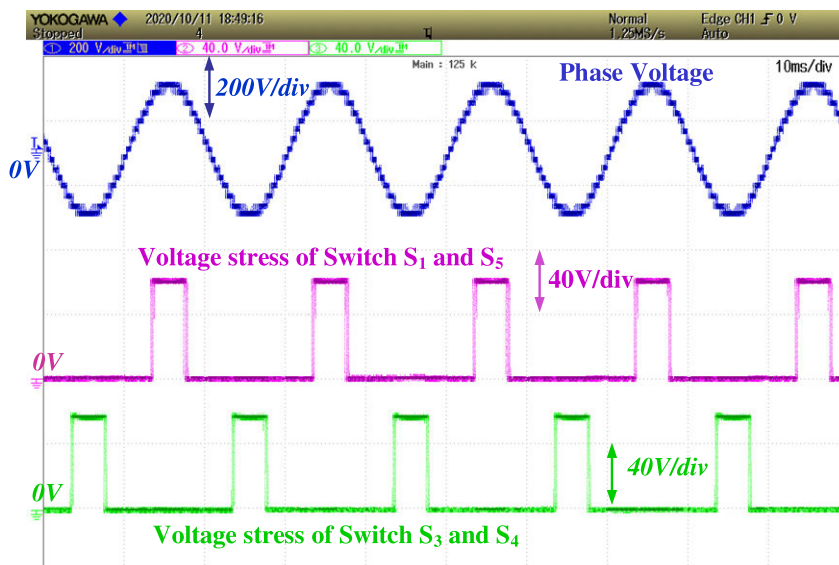


FIGURE 8. Experimental result of output voltage and voltage stress of switches ( $S_1, S_5$ ) and ( $S_3, S_4$ ).



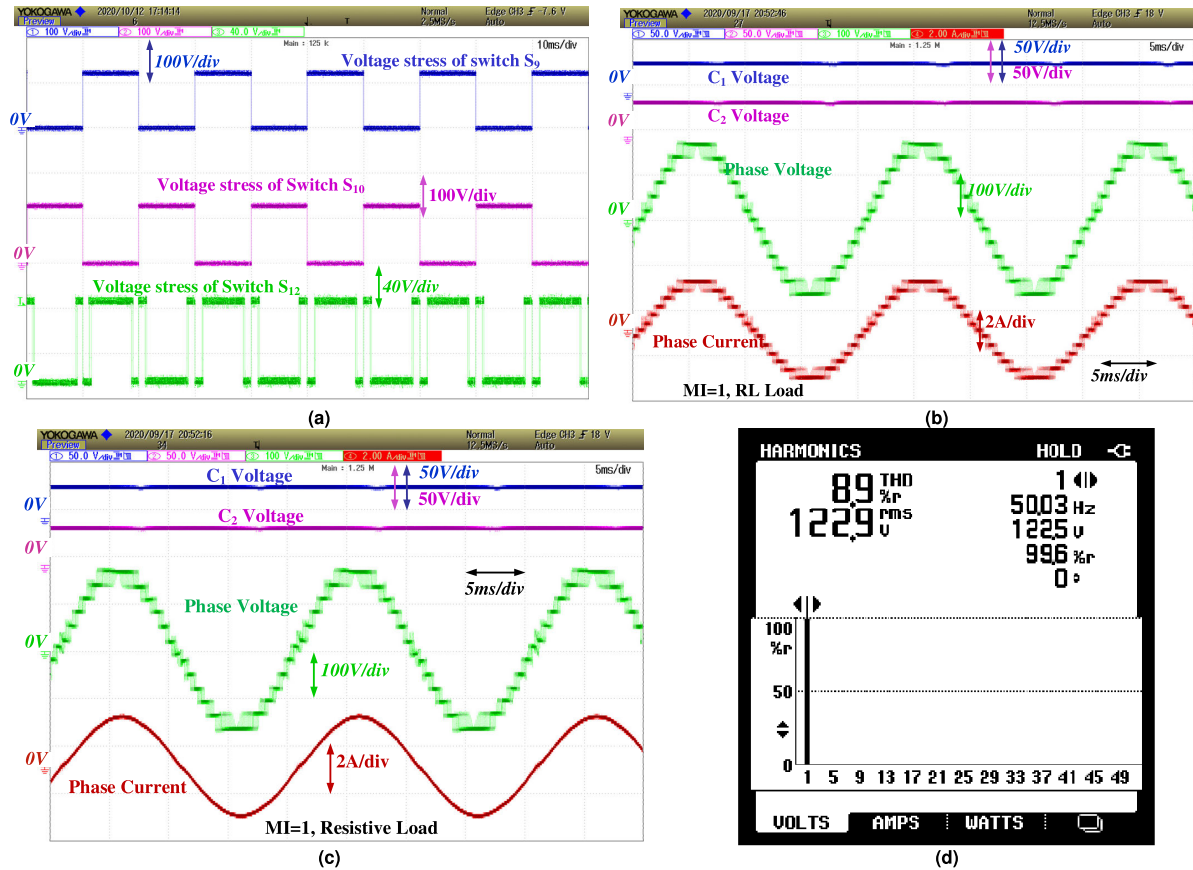


FIGURE 9. Experimental results with (a) voltage stress of switches,  $S_9$ ,  $S_{10}$ ,  $S_{12}$ , (b) R-load, (c) RL load, and (d) harmonic spectrum of output voltage.

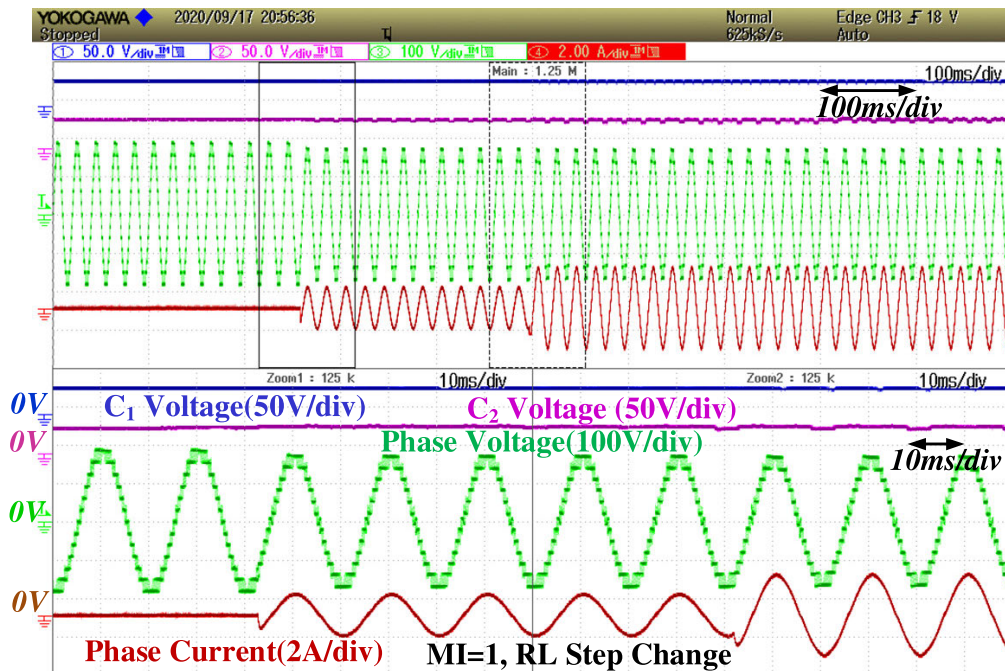
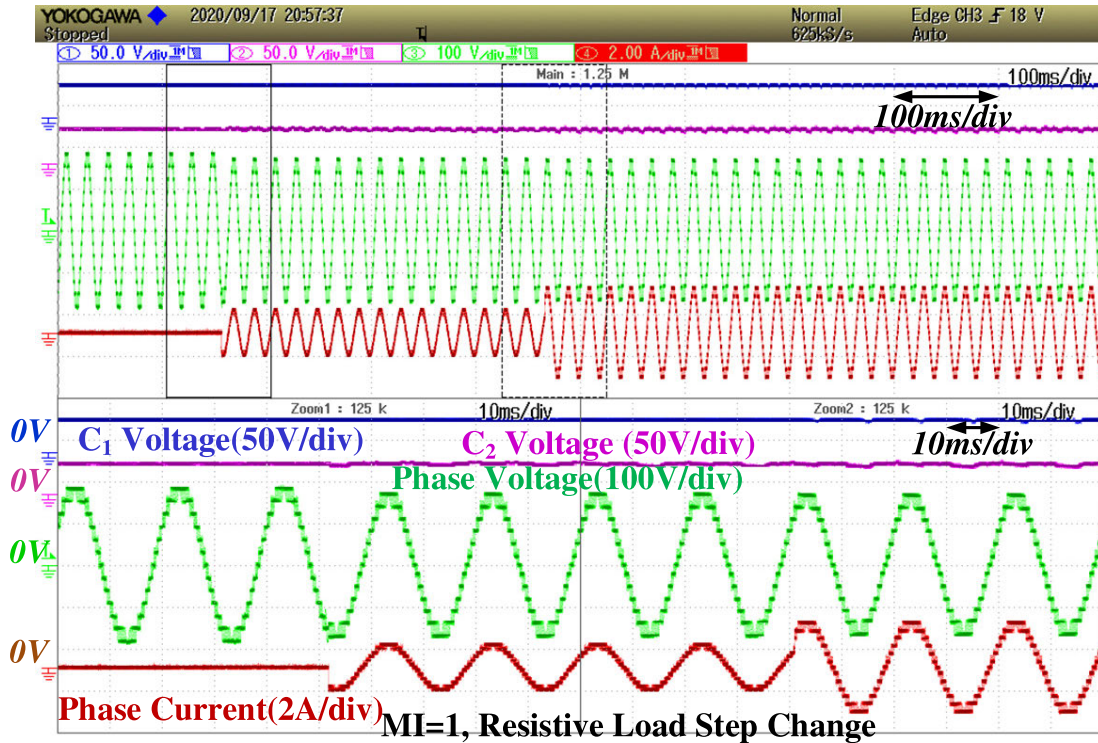


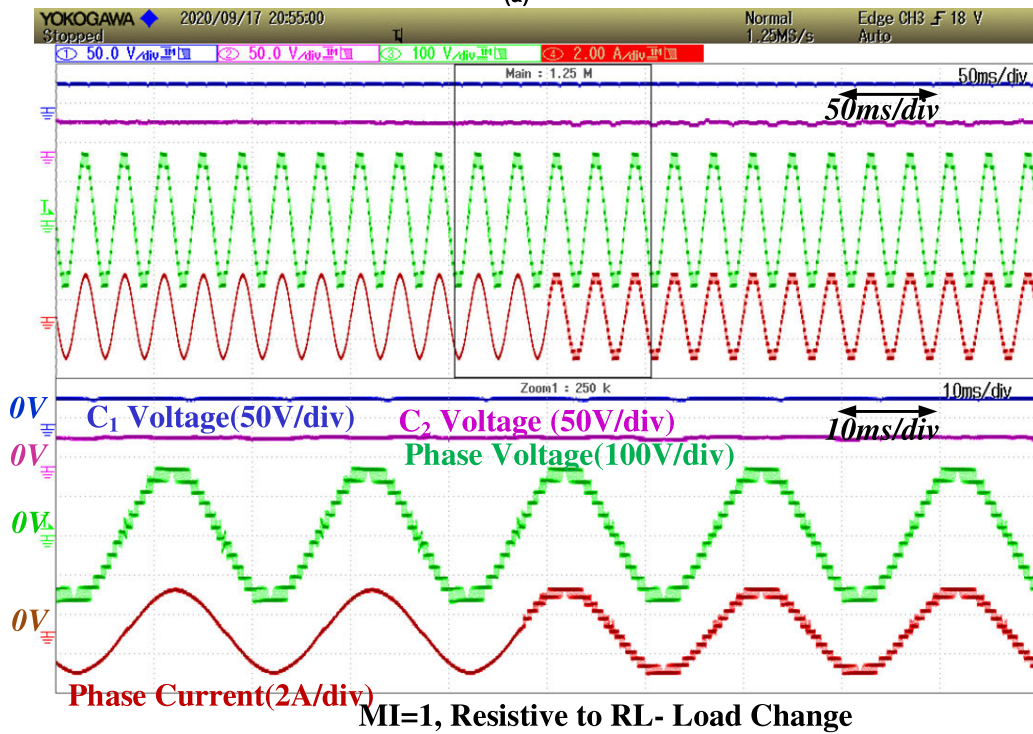
FIGURE 10. Experimental results with change in RL load.

in Fig. 11 (a). In the bottom side of this figure, a zoomed version of experimental results for the step change of R load from no-load to 180  $\Omega$  (series of two 90  $\Omega$  resistors) and

180  $\Omega$  to 90  $\Omega$  are shown, i.e., left and right respectively. The peak current magnitude is 0, 1A, and 2A for no-load, 180  $\Omega$  and 90  $\Omega$  respectively.



(a)



(b)

FIGURE 11. Experimental results with change in (a) R load and (b) load pf.

The proposed MLI is tested for a step-change in load type from RL to R, the results are shown in Fig. 11 (b). In this figure, it is clear that the change in the type of load RL to R results in a change in power factor, i.e.,  $\cos(X_L/R)$  for RL load and 1.0 for R load.

The experimental results of symmetrical source driven proposed MLI with the change in modulation index have shown in Fig. 12 (a). In this figure, the step change in MI is applied from 1 to 0.75, 0.75 to 0.5, 0.5 to 0.25. This results in the reduction of output voltage as well as current magnitudes



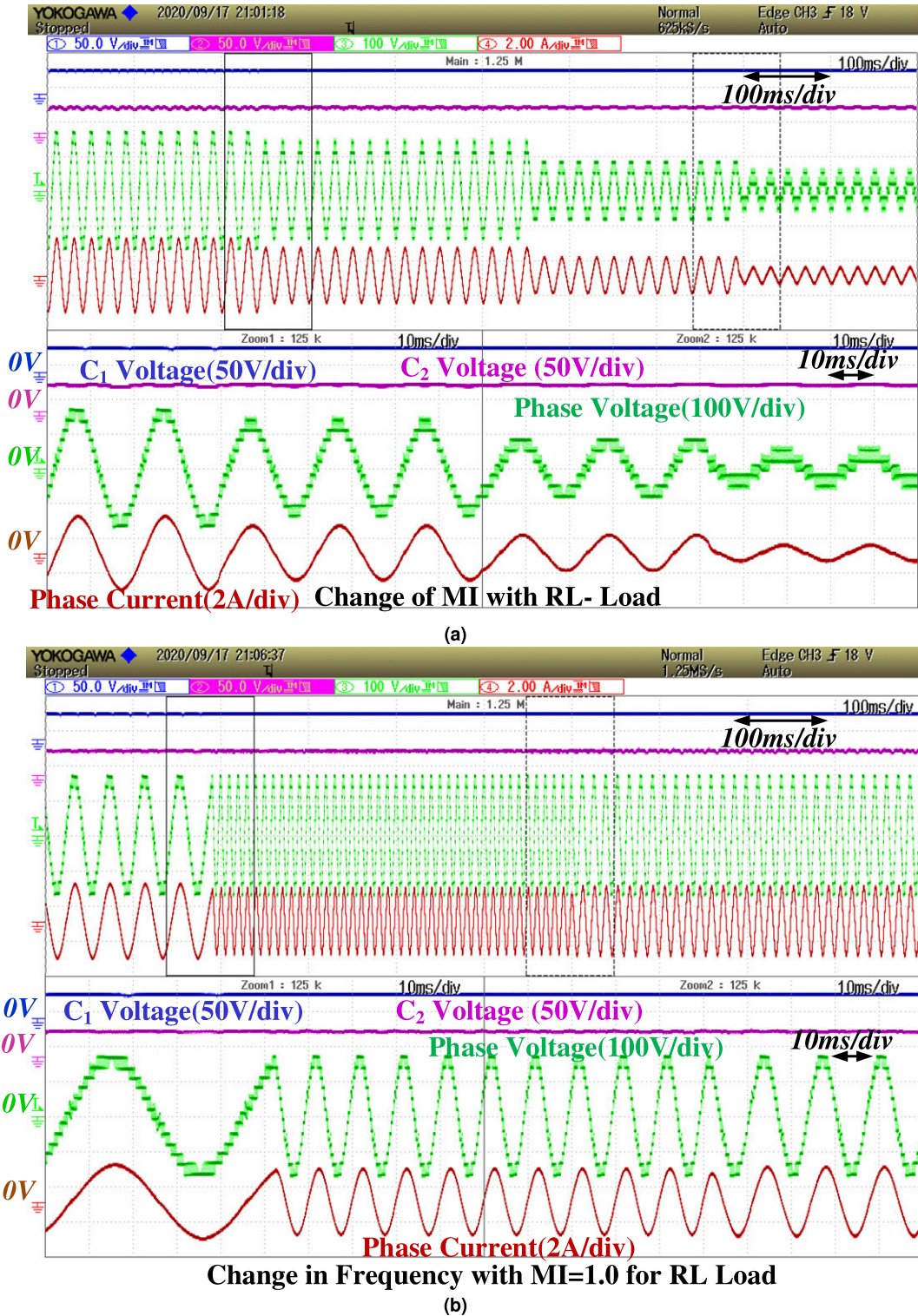


FIGURE 12. Experimental result with change in (a) output voltage frequency and (b) MI.

in proportional to the MI, which is clearly observed from Fig. 12 (a). The number of levels in the output voltage is also coming down gradually in accordance with the reduction in MI. On the bottom side of this figure, a zoomed version

of step-change in 1 to 0.75 and 0.75 to 0.5 are shown. The proposed MLI is also tested for a step-change in frequency operation at MI = 1, i.e., 25Hz, 100Hz, and 75Hz, the results are shown in Fig. 12 (b). The 50 Hz operation of

the proposed MLI results is already shown in Fig. 8 to Fig. 12. All these experimental results are evidence that the capacitors are inherently balanced for step-change in load type, load magnitude, MI, and frequency.

## V. CONCLUSION

In this paper, a new family of dual input-driven multilevel inverters with the integration of switched-capacitor units for attaining the boost capability as well as multilevel voltage has been discussed. For this, various multilevel inverters have been analyzed with the symmetrical/asymmetrical dc sources as well as different switched capacitor arrangements, and the detailed pros and cons of all configurations are presented. The higher voltage level generation, step-up operation, and lower voltage stress of the switches have been the main features of the proposed topologies. The comparative analysis is provided to highlight the benefits of the proposed topologies over the various multilevel inverters present in the literature. To show the effectiveness of the proposed topologies, a laboratory prototype of PT-I with the symmetrical sources is designed in the laboratory which will produce 13 levels and associated experimental results are provided. Different real-time operating conditions (like a step change in load, power factor, MI, and frequency) have been tested with the proposed topology and the experimental results show good agreement with the simulation results.

## REFERENCES

- [1] B. P. Reddy, M. A. Rao, M. Sahoo, and S. Keerthipati, "A fault-tolerant multilevel inverter for improving the performance of a pole-phase modulated nine-phase induction motor drive," *IEEE Trans. Ind. Electron.*, vol. 65, no. 2, pp. 1107–1116, Feb. 2018.
- [2] M. Rawa, M. D. Siddique, S. Mekhilef, N. M. Shah, H. Bassi, M. Seyedmahmoudian, B. Horan, and A. Stojcevski, "Dual input switched-capacitor-based single-phase hybrid boost multilevel inverter topology with reduced number of components," *IET Power Electron.*, vol. 13, no. 4, pp. 881–891, 2020.
- [3] P. R. Bana, K. P. Panda, R. T. Naayagi, P. Siano, and G. Panda, "Recently developed reduced switch multilevel inverter for renewable energy integration and drives application: Topologies, comprehensive analysis and comparative evaluation," *IEEE Access*, vol. 7, pp. 54888–54909, 2019.
- [4] J. S. M. Ali and V. Krishnaswamy, "An assessment of recent multilevel inverter topologies with reduced power electronics components for renewable applications," *Renew. Sustain. Energy Rev.*, vol. 82, no. 3, pp. 3379–3399, Feb. 2018.
- [5] B. P. Reddy and S. Keerthipati, "A multilevel inverter configuration for an open-end-winding pole-phase-modulated-multiphase induction motor drive using dual inverter principle," *IEEE Trans. Ind. Electron.*, vol. 65, no. 4, pp. 3035–3044, Apr. 2018.
- [6] M. D. Siddique, S. Mekhilef, N. M. Shah, A. Sarwar, A. Iqbal, M. Tayyab, and M. K. Ansari, "Low switching frequency based asymmetrical multilevel inverter topology with reduced switch count," *IEEE Access*, vol. 7, pp. 86374–86383, 2019.
- [7] M. D. Siddique, S. Mekhilef, N. M. Shah, N. Sandeep, J. S. M. Ali, A. Iqbal, M. Ahmed, S. S. M. Ghoneim, M. M. Al-Harathi, B. Alamri, F. A. Salem, and M. Orabi, "A single DC source nine-level switched-capacitor boost inverter topology with reduced switch count," *IEEE Access*, vol. 8, pp. 5840–5851, 2020.
- [8] J. Venkataramanaiah, Y. Suresh, and A. K. Panda, "A review on symmetric, asymmetric, hybrid and single DC sources based multilevel inverter topologies," *Renew. Sustain. Energy Rev.*, vol. 76, pp. 788–812, Sep. 2017.
- [9] R. S. Alishah, S. H. Hosseini, E. Babaei, and M. Sabahi, "Optimal design of new cascaded switch-ladder multilevel inverter structure," *IEEE Trans. Ind. Electron.*, vol. 64, no. 3, pp. 2072–2080, Mar. 2017.
- [10] R. S. Alishah, S. H. Hosseini, E. Babaei, M. Sabahi, and A. Z. Gharehkhoushan, "Optimal design of new cascade multilevel converter topology based on series connection of extended sub-multilevel units," *IET Power Electron.*, vol. 9, no. 7, pp. 1341–1349, 2016.
- [11] M. D. Siddique, S. Mekhilef, N. M. Shah, and M. A. Memon, "Optimal design of a new cascaded multilevel inverter topology with reduced switch count," *IEEE Access*, vol. 7, pp. 24498–24510, 2019.
- [12] M. D. Siddique, S. Mekhilef, N. M. Shah, J. S. M. Ali, M. Meraj, A. Iqbal, and M. A. Al-Hitmi, "A new single phase single switched-capacitor based nine-level boost inverter topology with reduced switch count and voltage stress," *IEEE Access*, vol. 7, pp. 174178–174188, 2019.
- [13] B. P. Reddy, M. D. Siddique, A. Iqbal, S. Mekhilef, S. Rahman, and P. K. Maroti, "7L-SCBI topology with minimal semiconductor device count," *IET Power Electron.*, vol. 13, no. 14, pp. 3065–3071, Nov. 2020.
- [14] M. D. Siddique, J. S. M. Ali, S. Mekhilef, A. Mustafa, N. Sandeep, and D. Almakhles, "Reduce switch count based single source 7L boost inverter topology," *IEEE Trans. Circuits Syst. I, Reg. Papers*, vol. 67, no. 12, pp. 3252–3256, Dec. 2020.
- [15] B. P. Reddy, M. D. Siddique, A. Iqbal, S. Mekhilef, S. Rahman, and P. K. Maroti, "7L-SCBI topology with minimal semiconductor device count," *IET Power Electron.*, vol. 13, no. 14, pp. 3199–3203, 2020.
- [16] P. Panda, P. R. Bana, and G. Panda, "A switched-capacitor self-balanced high-gain multilevel inverter employing a single DC source," *IEEE Trans. Circuits Syst. I, Reg. Papers*, vol. 67, no. 12, pp. 3192–3196, Dec. 2020.
- [17] X. Sun, B. Wang, Y. Zhou, W. Wang, H. Du, and Z. Lu, "A single DC source cascaded seven-level inverter integrating switched-capacitor techniques," *IEEE Trans. Ind. Electron.*, vol. 63, no. 11, pp. 7184–7194, Nov. 2016.
- [18] J. S. M. Ali and V. Krishnasamy, "Compact switched capacitor multilevel inverter (CSCMLI) with self-voltage balancing and boosting ability," *IEEE Trans. Power Electron.*, vol. 34, no. 5, pp. 4009–4013, May 2019.
- [19] N. Sandeep and U. R. Yarangatti, "A switched-capacitor-based multilevel inverter topology with reduced components," *IEEE Trans. Power Electron.*, vol. 33, no. 7, pp. 5538–5542, Jul. 2018.
- [20] A. Taghvaie, J. Adabi, and M. Rezaeejad, "A multilevel inverter structure based on a combination of switched-capacitors and DC sources," *IEEE Trans. Ind. Informat.*, vol. 13, no. 5, pp. 2162–2171, Oct. 2017.
- [21] E. Samadaei, M. Kaviani, and K. Bertilsson, "A 13-levels module (K-type) with two DC sources for multilevel inverters," *IEEE Trans. Ind. Electron.*, vol. 66, no. 7, pp. 5186–5196, Jul. 2019.
- [22] M. D. Siddique, S. Mekhilef, A. Sarwar, A. Alam, and N. Mohamed Shah, "Dual asymmetrical DC voltage source based switched capacitor boost multilevel inverter topology," *IET Power Electron.*, vol. 13, no. 7, pp. 1481–1486, 2020.
- [23] R. S. Alishah, S. H. Hosseini, E. Babaei, M. Sabahi, and A. Zare, "Extended high step-up structure for multilevel converter," *IET Power Electron.*, vol. 9, no. 9, pp. 1894–1902, Jul. 2016.
- [24] R. Barzegarkhoo, H. M. Kojabadi, E. Zamiri, N. Vosoughi, and L. Chang, "Generalized structure for a single phase switched-capacitor multilevel inverter using a new multiple DC link producer with reduced number of switches," *IEEE Trans. Power Electron.*, vol. 31, no. 8, pp. 5604–5617, Aug. 2016.
- [25] E. Zamiri, N. Vosoughi, S. H. Hosseini, R. Barzegarkhoo, and M. Sabahi, "A new cascaded switched-capacitor multilevel inverter based on improved series-parallel conversion with less number of components," *IEEE Trans. Ind. Electron.*, vol. 63, no. 6, pp. 3682–3694, Jun. 2016.
- [26] M. D. Siddique, S. Mekhilef, A. Sarwar, A. Alam, and N. M. Shah, "Dual asymmetrical DC voltage source based switched capacitor boost multilevel inverter topology," *IET Power Electron.*, vol. 13, no. 7, pp. 1481–1486, 2020.
- [27] S. R. Raman, K. W. E. Cheng, and Y. Ye, "Multi-input switched-capacitor multilevel inverter for high-frequency AC power distribution," *IEEE Trans. Power Electron.*, vol. 33, no. 7, pp. 5937–5948, Jul. 2018.
- [28] Y. C. Fong, S. R. Raman, Y. Ye, and K. W. E. Cheng, "Generalized topology of a hybrid switched-capacitor multilevel inverter for high-frequency AC power distribution," *IEEE J. Emerg. Sel. Topics Power Electron.*, vol. 8, no. 3, pp. 2886–2897, Sep. 2020.
- [29] S. S. Lee, K.-B. Lee, I. M. Alsofyani, Y. Bak, and J. F. Wong, "Improved switched-capacitor integrated multilevel inverter with a DC source string," *IEEE Trans. Ind. Appl.*, vol. 55, no. 6, pp. 7368–7376, Nov./Dec. 2019.
- [30] R. Barzegarkhoo, M. Moradzadeh, E. Zamiri, H. M. Kojabadi, and F. Blaabjerg, "A new boost switched-capacitor multilevel converter with reduced circuit devices," *IEEE Trans. Power Electron.*, vol. 33, no. 8, pp. 6738–6754, Aug. 2018.



- [31] R. Barzegarkhoo, E. Zamiri, M. Moradzadeh, and H. Shadabi, "Symmetric hybridised design for a novel step-up 19-level inverter," *IET Power Electron.*, vol. 10, no. 11, pp. 1377–1391, 2017.
- [32] M. D. Siddique, S. Mekhilef, S. Padmanaban, M. A. Memon, and C. Kumar, "Single phase step-up switched-capacitor based multilevel inverter topology with SHEPWM," *IEEE Trans. Ind. Appl.*, early access, Jun. 12, 2020, doi: [10.1109/TIA.2020.3002182](https://doi.org/10.1109/TIA.2020.3002182).



**ATIF IQBAL** (Senior Member, IEEE) received the B.Sc. degree and the M.Sc. degrees in power system and drives engineering from Aligarh Muslim University (AMU), Aligarh, India, in 1991 and 1996, respectively, and the Ph.D. degree from Liverpool John Moores University, Liverpool, U.K., in 2006. He has been employed as a Lecturer with the Department of Electrical Engineering, AMU, since 1991, where he served as a Full Professor until August 2016. He has published widely in international journals and conferences his research findings related to Power Electronics and Renewable Energy Sources. He has authored or coauthored more than 300 research articles and one book and three chapters in two other books. He has supervised several large research and development projects. His research interests include modeling and simulation of power electronic converters, control of multi-phase motor drives, and renewable energy sources. He became a Fellow IET, U.K., in 2018, a Fellow IE, India, in 2012, and an Associate Editor IEEE TRANSACTIONS ON INDUSTRY APPLICATION, the Editor-in-Chief, *I-manager's Journal on Electrical Engineering*, an Associate Professor at Electrical Engineering, Qatar University, and a Former Full Professor at Electrical Engineering, Aligarh Muslim University (AMU), Aligarh, India. He was a recipient of the Outstanding Faculty Merit Award AY from 2014 to 2015 and the Research Excellence Award at Qatar University, Doha, Qatar. He was also a recipient of the Maulana Tufail Ahmad Gold Medal for standing first at B.Sc. Engg., exams from AMU, in 1991. He has received the best research papers awards at IEEE ICIT-2013, IET-SESICON-2013, and SIGMA 2018.



**MARIF DAULA SIDDIQUE** (Member, IEEE) was born in Chhapra, Bihar, India, in 1992. He received the B.Tech. and M.Tech. degrees in electrical engineering from Aligarh Muslim University (AMU), in 2014 and 2016, respectively. He is currently pursuing the Ph.D. degree with the Power Electronics and Renewable Energy Research Laboratory (PEARL), Department of Electrical Engineering, University of Malaya, Kuala Lumpur, Malaysia. He is also working as a Research Assistant with

the Department of Electrical Engineering, Qatar University, Doha, Qatar. He has authored or coauthored more than 35 publications in international journals and conference proceedings. His research interests include step-up power electronics converters (dc/ac and dc/dc), multilevel inverter topologies and their control. He is serving as a Regular Reviewer for various journals of IEEE and IET.



**B. PRATHAP REDDY** (Member, IEEE) received the B.Tech. degree in electrical and electronics engineering from the Gates Institute of Technology, Jawaharlal Nehru Technological University, Anantapur, in 2014, the M.Tech. degree in power electronics and drives from Lovely Professional University, Punjab, India, in 2016, and the Ph.D. degree in power electronics and drives from the Indian Institute of Technology Hyderabad, India, in 2019. He has been as a Postdoctoral Research Fellow with the Department of Electrical Engineering, Qatar University, Qatar, since May 2019. His research interests include pole phase modulation techniques for electric drives, multilevel inverters, multiphase machines, DC–DC converters, open-end winding induction motor drives, and pulse width modulation techniques. He received the Gold Medal for scoring the highest CGPA and Academic Honour Award in M.Tech. from Lovely Professional University, in 2016. During his Ph.D., received the Excellence in Research Award, Appreciation in Research awards for the year 2018 and 2019, respectively, at IIT Hyderabad, India.



**PANDAV KIRAN MAROTI** (Member, IEEE) received the bachelor's degree in electronics and telecommunication from Dr. Babasaheb Ambedkar Marathwada University, Aurangabad, India, in 2011, the M.Tech. degree (Hons.) in power electronics and drives from the Vellore Institute of Technology, Vellore, India, in 2014, and the Ph.D. degree in power electronics from the University of Johannesburg, South Africa, under the guidance of Prof. S. Padmanaban (Senior Member, IEEE) and co-guide Prof. F. Blaabjerg (Power Electronics President of IEEE and Fellow, IEEE). He was working as an Assistant Professor with the Marathwada Institute of Technology, Aurangabad, Maharashtra, India, from 2014 to 2016. He is currently a Visiting Researcher with Qatar University. He has published scientific articles in the field of Power Electronics (multilevel DC/DC and DC/AC converter, multiphase open winding inverter). He also received GLOBAL EXPERIENCE SCHOLARSHIP (GES). He received the Best Paper Award from ETAEERE in 2016 sponsored Lecture note in Electrical Engineering, Springer book series. He is a professional active member of Industrial Electronics, Power Electronics, Industrial Application, and Young Professionals societies. Also, he is active Reviewer Member of various reputed international conferences and journal, including IEEE and IET.



**RASHID ALAMMARI** (Senior Member, IEEE) received the B.S. degree from Qatar University in 1985, the M.Sc. degree from Washington State University, Pullman, WA, USA, in 1989, and the Ph.D. degree from Strathclyde University, Glasgow, U.K., in 1996, all in electrical engineering, majoring in power systems. He started as a Teaching Assistant with an industry experience partnership with the Ministry of Electricity and Water. He became an Assistant Professor in 1996, and was promoted to an Associate Professor in 2003. He was appointed as the Head of the QU Foundation Program from 1998 to 2000, then as the Chairman of the Department of Electrical Engineering from 2000 to 2004, leading the Department to its first ABET accreditation. He was appointed as the Dean of the College of Engineering, Qatar University, from October 2012 to March 2016. He is a published author of many academic studies on power systems and power quality. He received the University Distinguished Faculty Research Award in 2004 and in 2012 achieved the State of Qatar Incentive Award in Electrical Engineering. He got a scholarship from Qatar University.

...